



HAL
open science

Dynamical footprints of Hurricanes in the Tropical Dynamics

Davide Faranda, Gabriele Messori, Pascal Yiou, Soulivanh Thao, Flavio Pons,
Berengere Dubrulle

► **To cite this version:**

Davide Faranda, Gabriele Messori, Pascal Yiou, Soulivanh Thao, Flavio Pons, et al.. Dynamical footprints of Hurricanes in the Tropical Dynamics. *Chaos: An Interdisciplinary Journal of Nonlinear Science*, In press. hal-03219409v3

HAL Id: hal-03219409

<https://hal.science/hal-03219409v3>

Submitted on 28 Sep 2022 (v3), last revised 7 Dec 2022 (v4)

HAL is a multi-disciplinary open access archive for the deposit and dissemination of scientific research documents, whether they are published or not. The documents may come from teaching and research institutions in France or abroad, or from public or private research centers.

L'archive ouverte pluridisciplinaire **HAL**, est destinée au dépôt et à la diffusion de documents scientifiques de niveau recherche, publiés ou non, émanant des établissements d'enseignement et de recherche français ou étrangers, des laboratoires publics ou privés.

1 Dynamical footprints of Hurricanes in the Tropical Dynamics

2 D. Faranda,^{1,2,3, a)} G. Messori,^{4,5} P. Yiou,¹ S. Thao,¹ F. Pons,¹ and B. Dubrulle⁶

3 ¹⁾*Laboratoire des Sciences du Climat et de l'Environnement,*
4 *UMR 8212 CEA-CNRS-UVSQ, Université Paris-Saclay & IPSL,*
5 *CE Saclay l'Orme des Merisiers, 91191, Gif-sur-Yvette, France*

6 ²⁾*London Mathematical Laboratory, 8 Margravine Gardens, London, W6 8RH,*
7 *UK*

8 ³⁾*LMD/IPSL, Ecole Normale Supérieure, PSL research University, 75005, Paris,*
9 *France*

10 ⁴⁾*Department of Earth Sciences and Centre of Natural Hazards*
11 *and Disaster Science (CNDS), Uppsala University, Uppsala,*
12 *Sweden*

13 ⁵⁾*Department of Meteorology and Bolin Centre for Climate Research,*
14 *Stockholm University, Stockholm, Sweden.*

15 ⁶⁾*SPEC, CEA, CNRS, Université Paris-Saclay, F-91191 CEA Saclay, Gif-sur-Yvette,*
16 *France.*

17 (Dated: 28 September 2022)

18 Hurricanes — and more broadly tropical cyclones — are high-impact weather phenomena
19 whose adverse socio-economic and ecosystem impacts affect a considerable part of the
20 global population. Despite our reasonably robust meteorological understanding of tropical
21 cyclones, we still face outstanding challenges for their numerical simulations. Conse-
22 quently, future changes in the frequency of occurrence and intensity of tropical cyclones
23 are still debated. Here, we diagnose possible reasons for the poor representation of tropical
24 cyclones in numerical models, by considering the cyclones as chaotic dynamical systems.
25 We follow 197 tropical cyclones which occurred between 2010 and 2020 in the North At-
26 lantic using the HURDAT2 and ERA5 datasets. We measure the cyclones instantaneous
27 number of active degrees of freedom (local dimension) and the persistence of their sea-
28 level pressure and potential vorticity fields. During the most intense phases of the cyclones,
29 and specifically when cyclones reach hurricane strength, there is a collapse of degrees of
30 freedom and an increase in persistence. The large dependence of hurricanes dynamical
31 characteristics on intensity suggests the need for adaptive parametrisation schemes which
32 take into account the dependence of the cyclone’s phase, in analogy with high-dissipation
33 intermittent events in turbulent flows.

^{a)}Correspondence to davide.faranda@lscce.ipsl.fr

34 I. LEAD PARAGRAPH

35 **Tropical cyclones are both high-impact weather events and challenging phenomena from**
36 **the point of view of numerical modelling. While their lifecycle is relatively well understood,**
37 **there are still difficulties in the representation of their dynamics in weather and climate mod-**
38 **els, and in drawing robust conclusions on how different climate conditions may affect their**
39 **frequency of occurrence and intensity. Here, we consider tropical cyclones as chaotic dynam-**
40 **ical systems. We show that the formation of particularly intense cyclones, termed hurricanes**
41 **in the North Atlantic, coincides with a reduction of the phase space of the atmospheric dy-**
42 **namics to a low-dimensional and persistent object, where few rotational kinetic degrees of**
43 **freedom dominate the dynamics. This suggests the need for adaptive parameterisations to**
44 **integrate the governing equations when simulating intense tropical cyclones in numerical**
45 **climate models.**

46 II. INTRODUCTION

47 Tropical cyclones are high-impact extreme weather events. For example, they are the costli-
48 est natural disaster category in the United States^{1,2}, with the damage related to hurricane Katrina
49 (2005) alone amounting to about 1% of the gross domestic product of the country². Trends in
50 the frequency of occurrence and intensity of tropical cyclones are difficult to discern in observa-
51 tions because of their relative rarity and of the brevity of highly spatially and temporally resolved
52 datasets, which rely on satellite observations³. Projections of future climates indicate an increase
53 in the intensity of tropical cyclones in the North Atlantic sector, albeit only with medium confi-
54 dence⁴. Indeed, reproducing the dynamics of the most severe events is difficult even in the most
55 advanced global or regional climate models⁵. For example, while mid-latitude synoptic dynamics
56 mostly originate from the chaotic structure of the motions associated with baroclinic instability^{6,7},
57 tropical cyclones are characterized by a rapid organization of convectively unstable flows whose
58 dynamics is turbulent and highly sensitive to boundary conditions⁸. To understand the reasons
59 for the poor representation of tropical cyclones in numerical models, we adopt a dynamical sys-
60 tem methodology which represents the cyclones as states of a chaotic, high-dimensional system.
61 We specifically compute two metrics reflecting instantaneous properties of the cyclones, namely
62 persistence and local dimension. Local dimension is a proxy for the system's number of active

63 degrees of freedom, and can be linked to the system’s predictability^{9–11}. Persistence provides in-
64 formation about the dominant time scale of the dynamics. Both metrics may easily be applied
65 to large datasets, such as climate reanalyses. They have recently provided insights on a number
66 of geophysical phenomena, including transitions between transient metastable states of the mid-
67 latitude atmosphere^{9,12}, palaeoclimate attractors^{13,14}, slow earthquake dynamics¹⁵ and changes in
68 mid-latitude atmospheric predictability under global warming¹⁶.

69 All these applications have taken an Eulerian point-of-view, focusing on a fixed spatio-temporal
70 domain. Here, we provide the first application of the two metrics from a (semi)-Lagrangian per-
71 spective, by computing the persistence and local dimension of tropical cyclones which we track in
72 space and time. This approach is particularly suited to study the complex behavior of convectively
73 unstable flow systems (see, e.g., ¹⁷ and chapter 12 in¹⁸). After putting the tropical cyclones in
74 the dynamical system framework, we may investigate whether they act as generic points of the
75 phase space or whether their dynamics exhibits a peculiar behavior. In the first case, the numerical
76 parametrizations developed for generic tropical climate states should work well when applied to
77 small-scale features of tropical cyclones. In the second case, cyclones dynamical properties are
78 dependent on their phase, so that leading parametrizations designed for generic tropical dynamical
79 states will not work properly on cyclones.

80 In the rest of the study, we compute the persistence and local dimension of tropical cyclones,
81 and use these to outline a strategy to improve their numerical simulation.

82 **III. OBSERVABLES FOR CYCLONE DYNAMICS**

83 The historical cyclone data are the "best track data" from the Atlantic HURDAT2 database¹⁹,
84 developed by the National Hurricane Center. This database provides, amongst other variables,
85 the location of tropical cyclones, their maximum winds, central pressure and categorisation. The
86 values are obtained as a post-storm analysis of all available data, collected both remotely and in-
87 situ. We specifically consider separately hurricanes (HU), tropical storms (TS) and post-tropical
88 cyclones associated with an extratropical transition (EX). We further use instantaneous potential
89 vorticity (PV) at 500 hPa and sea-level pressure (SLP) data from ECMWF’s ERA5 reanalysis²⁰.
90 For both datasets we make use of 6-hourly data, and additionally data at the time when the HUR-
91 DAT2 database displays a cyclone landfall; the ERA5 data is retrieved at a horizontal resolution
92 of 0.25°.

93 Our analysis includes all tropical cyclones classified in HURDAT2 from 2010 to 2020 included.
 94 We use semi-Lagrangian observables, i.e. we select a horizontal domain around the tropical cyclo
 95 location, of size $\sim 1200 \times 1200$ km (41×41 grid points in ERA5). The choice of SLP is motivated
 96 by its widespread use in hurricane tracking²¹ and the fact that it is a first approximation of the
 97 horizontal velocity streamfunction. The PV is often used in the study of tropical cyclones and
 98 relates to their intensification and symmetry structure^{22,23}, and takes explicitly into account the
 99 strength of the cyclones warm core. Indeed, PV may be viewed as a metric of latent heat release
 100 and therefore of the intensity of the diabatic processes taking place in the tropical cyclones (cloud
 101 formation, precipitation)^{24,25}. We specifically select mid-level PV, following for example^{26,27}.
 102 As control parameter, we chose the maximum winds from HURDAT2, since this quantity can be
 103 directly connected to the economic loss caused by tropical cyclones²⁸.

104 IV. A DYNAMICAL SYSTEMS VIEW OF TROPICAL CYCLONES

105 We follow tropical cyclones in phase space as states of a chaotic, high-dimensional dynamical
 106 system. Each instantaneous state of the cyclone, as represented by a given atmospheric variable,
 107 corresponds to a point in a reduced phase space (namely a special Poincaré section). We sample
 108 these states at discrete points i , determined by the temporal resolution of the HURDAT2 data,
 109 that is every 6h or whenever the HURDAT2 database displays a cyclone landfall. Our aim is
 110 to diagnose the dynamical properties of the instantaneous (in time) and local (in phase-space)
 111 states of the cyclone, as represented by the chosen atmospheric variable and geographical domain
 112 (physical space in Fig. 1). To do so, we leverage two metrics issuing from the combination of
 113 extreme value theory with Poincaré recurrences^{29–31}. We consider the ensemble $\{X_i\}$, which in
 114 our analysis are SLP or PV maps of all timesteps i for all tropical cyclones in our dataset, always
 115 centred on the cyclones location. We further consider a state of interest ζ , which would correspond
 116 to a single SLP or PV map drawn from this dataset. We then define logarithmic returns as:

$$117 \quad g(X_i, \zeta) = -\log[\text{dist}(X_i, \zeta)] \quad (1)$$

118 Here, "dist" is the Euclidean distance between pairs of SLP or PV maps, but more generally it
 119 can be any distance function between two vectors which tends to zero as the two vectors increas
 120 ingly resemble each other. We thus have a time series g of logarithmic returns which is large at
 121 times i when X_i is close to ζ .

122 We next define exceedances as $\{u(\zeta) = g(X_i, \zeta) - s(q, \zeta) \forall i : g(X_i, \zeta) > s(q, \zeta)\}$, where
 123 $s(q, \zeta)$ is a high threshold corresponding to the q th quantile of $g(X_i, \zeta)$. These are effectively
 124 the previously-mentioned Poincaré recurrences, for the chosen state ζ (phase space in Fig. 1).
 125 The Freitas-Freitas-Todd theorem^{29,30} states that the cumulative probability distribution $F(u(\zeta))$
 126 is approximated by the exponential member of the Generalised Pareto Distribution. We thus have
 127 that:

$$128 \quad F(u, \zeta) \simeq \exp \left[-\vartheta(\zeta) \frac{u(\zeta)}{\sigma(\zeta)} \right] \quad (2)$$

129 The parameters u , namely the exceedances, and σ , namely the scale parameter of the Gener-
 130 alised Pareto Distribution, depend on the chosen state ζ , while ϑ is the so-called extremal index,
 131 namely a measure of clustering³². We estimate it here using the Süveges Estimator³³.

132 From the above, we can define two dynamical systems metrics: local dimension (d) and per-
 133 sistence (θ^{-1}). The local dimension is given by $d(\zeta) = 1/\sigma(\zeta)$, with $0 < d \leq +\infty$. When X_i
 134 contains all the variables of the system, the estimation of d based on extreme value theory has a
 135 number of advantages over traditional methods (e.g. the box counting algorithm³⁴). First, it does
 136 not require to estimate the volume of different sets at different scales: the selection of $s(q)$ based
 137 on the quantile provides a selection of different thresholds s which depends on the recurrence rate
 138 around the point ζ . Moreover, it does not require the a-priori selection of the maximum embedding
 139 dimension, as the observable g is always a univariate time-series. Even when X_i does not contain
 140 all variables of the system, the estimation of d through extreme value theory is still a powerful tool
 141 to compare different states of high-dimensional chaotic systems³⁵.

142 The persistence of the state ζ is measured via the extremal index $0 < \vartheta(\zeta) < 1$. We define the
 143 inverse of the average residence time of trajectories around ζ as: $\theta(\zeta) = \vartheta(\zeta)/\Delta t$, with Δt being
 144 the timestep of the underlying data (here 6 hours). Since the extremal index is non-dimensional,
 145 $\theta(\zeta)$ has units of frequency. θ^{-1} is then a measure of persistence. If ζ is a fixed point of the
 146 attractor $\theta(\zeta) = 0$. For a trajectory that leaves the neighborhood of ζ at the next time iteration,
 147 $\theta = 1$. A caveat of our approach is that our dataset is constructed from a sequence of cyclones
 148 which is not continuous in space-time. This may introduce a bias in our calculation of θ if the final
 149 state of a cyclone is a recurrence of the initial state of the following cyclone. This is highly unlikely
 150 due to the very different nature of the growth versus weakening stages of tropical cyclones. We
 151 further note that this does not affect the computation of d , which is insensitive to time reshuffling.

152 While the derivation of d and θ^{-1} may seem very abstract, the two metrics can be related to

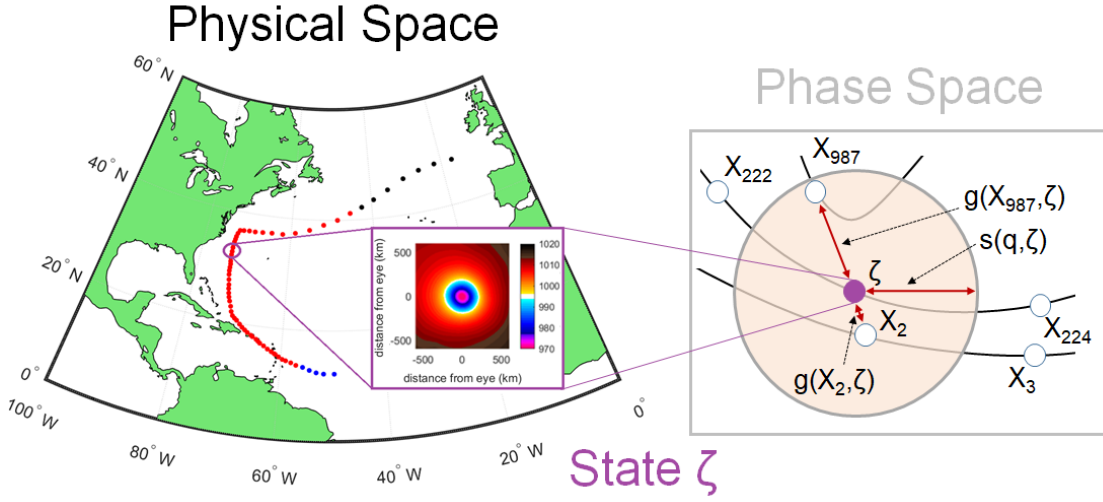


FIG. 1. Schematic of the computation of the dynamical systems metrics for an instantaneous state of a tropical cyclone. We take a snapshot of the cyclone in physical space (black quadrant), in this example a latitude-longitude map of sea-level pressure, which corresponds to state ζ in our reduced phase space. The right hand side panel shows the discrete sampling of the phase-space at points X_i (white circles). The shaded circle is a 2D representation of the hyper-sphere determined by the high threshold $s(q, \zeta)$, which defines recurrences. The logarithmic distances between measurements defined by $g(X_i, \zeta)$ are marked by double-headed arrows. For all points within the hyper-sphere, $g(X_i, \zeta) > s(q, \zeta)$ holds. In the schematic, only two measurements satisfy this condition (adapted from¹⁴).

153 the properties of the tropical cyclones. d is a proxy for the active number of degrees of freedom
 154 of the cyclones instantaneous states. On the other hand, θ^{-1} measures the persistence of such
 155 states and is related to the dominant time scale of the dynamics (the Lyapunov exponent³⁶). Both
 156 these quantities are known to be connected to the dynamical (Kolmogorov Sinai) entropy since the
 157 seminal work of Young³⁷.

158 V. DYNAMICAL PROPERTIES OF TROPICAL CYCLONES: COLLAPSE OF 159 DEGREES OF FREEDOM AND INCREASE IN PERSISTENCE IN INTENSE STORMS

160 Before focusing on the analysis of the dynamics of tropical cyclones specifically, we assess the
 161 peculiarity of their dynamical footprints when compared with a box of the tropical Atlantic ocean.
 162 We use ERA5 6h data for SLP and PV covering the period 2017-2021 and considered the squared

163 horizontal domain spanning $10N < \text{Latitude} < 20N$ $-50W < \text{Longitude} < 40W$. The results are shown in
 164 Figure 2. For SLP (Fig. 2a), that is the non cyclonic states do not feature any particular structure
 165 and they are characterized by non-persistent behavior ($\theta \lesssim 1$) and a range of dimensions similar to
 166 those of the tropical cyclones. For PV, at a first glance, there is no clear separation between control
 167 box and tropical cyclones of the distributions on the basis of the analysis of the diagrams (Fig. 2b)
 168 with d and θ spanning a similar range of values. On the other hand, the analysis of the violin
 169 plots presented in Fig. 2c-f) show that the distributions are different. To quantify this difference
 170 we apply a two-sided Cramer-von Mises test at the 0.05 significance level³⁸. The p-values found
 171 (virtually 0) imply that the null hypothesis that the two samples come from the same distribution
 172 can be rejected hinting to a statistically significant difference.

173 The previous analysis shows that the distribution of dynamical properties of tropical cyclones
 174 is significantly different from the one of a control box of Atlantic ocean. We now focus on the re-
 175 lationship between the dynamical indicators and the different tropical cyclones intensity measures.
 176 Figure 3a, b shows the values of dimension d and inverse persistence θ computed on SLP and 500
 177 hPa PV, with maximum winds in colours. The two local dimensions show different ranges, with
 178 $d_{SLP} < 30$ and d_{PV} attaining higher values. This reflects the fact that the PV dynamics involve
 179 multiple spatial scales, which reflect several underlying phenomena coming from convective and
 180 larger-scale aspects of cyclones and tropical dynamics, e.g. atmospheric waves³⁹. SLP, on the
 181 other hand, reflects the synoptic-scale structures ($\sim 10^3$ km). The range of local dimensions found
 182 is relatively low compared to the number of grid-points used, which is 41×41 . This means that
 183 the majority of the degrees of freedom are frozen when we follow coherent convective phenomena
 184 such as tropical cyclones. Moreover, lag-0 cross correlation coefficient between d_{SLP} and d_{PV} is
 185 0.23, suggesting that the two variables carry different information. The persistence range is also
 186 different for SLP and PV, with $0.1 < \theta_{SLP} < 1$ and $0.3 < \theta_{PV} < 0.8$. In units of time, these values
 187 indicate an SLP persistence between 6 and 60 hours and a PV persistence between 7.5 and 20
 188 hours. A timescale of 1–2.5 days is consistent with the synoptic-scale intensification of a cyclone,
 189 while timescales of a few hours to a day are consistent with changes in the convective structure of
 190 a cyclone. The lag-0 cross correlation coefficient between θ_{SLP} and θ_{PV} is 0.02, even
 191 lower than for d , again suggesting that the two carry different information.

192

193 We now connect the values of d and θ for SLP and PV to the underlying physics of the storms
 194 using the maximum wind speed. For SLP (Figure 3a) we note a strong dependence of θ on

195 the maximum winds. Low to moderate winds are associated with high θ , while stronger winds
196 correspond to lower θ . A weaker relation holds for d_{SLP} and maximum winds. For PV (Figure 3b),
197 strong winds match low d values and intermediate-to-high θ values. Thus, SLP suggests that
198 intense cyclones correspond to persistent states, while PV that they display a low local dimension
199 and intermediate-to-low persistence. Looking at the scatterplots and PDFs of the two dynamical
200 systems metrics conditioned on the HURDAT2 cyclone classification (Figure 3c, d), provides a
201 picture consistent with the above. For SLP, HU and EX display a markedly higher persistence
202 than TS. For PV, HU display a lower dimension and lower persistence than both TS and EX. The
203 medians of all PDFs are significantly different at the 1% level under a Wilcoxon rank sum test,
204 except for d_{SLP} for HU and EX (not shown). We interpret these dynamical system properties
205 as follows. When the storms produce strong winds and diabatic phenomena (HU with high PV
206 values and strong precipitation), the convective-scale dynamics collapses to an object with few
207 degrees of freedom (low d_{PV}), yet low persistence (high θ_{PV}). Nonetheless, the synoptic-scale
208 HU field is highly persistent (low θ_{SLP}), with values comparable to those of EX. SLP reflects a
209 quasi-symmetrical horizontal cyclonic structure, which for both HU and EX is characteristic of
210 the cyclone over an extended period of time. Weaker TS likely do not have a coherent cyclonic
211 core throughout their life cycle, as reflected in the high values of θ_{SLP} .

212 The mean SLP and PV footprints of the system are qualitatively similar across all three cy-
213 clone categories (Fig. 4), although EX show a larger spatial scale than both TS and HU. In all
214 three cases, the structures are roughly axisymmetric, showing that the EX cyclones included in
215 HURDAT2 still retain tropical-like characteristics. Clearer differences emerge when looking at the
216 standard deviation of the SLP and PV maps, computed at each gridpoint over all maps included
217 in our analysis (Fig. 5). Here, HU and TS show qualitatively similar, axisymmetric structures,
218 while EX show a clear meridional asymmetry in SLP and a less marked zonal asymmetry in PV.
219 Notwithstanding the broad similarity in mean structure between three cyclone categories, the dy-
220 namical systems metrics are nonetheless able to differentiate their characteristics. This suggests
221 that they sample from the systems dynamic variability and other subtle differences that do not
222 emerge from the composite maps, such as the evolution of the system mean structure during the
223 different phases of its lifecycle.

224

225 VI. DYNAMICAL SYSTEMS METRICS AND RAPID INTENSIFICATION

226 We now investigate whether the same dynamical systems framework can be used to investigate
227 rapid intensification. Rapid intensification occurs when a tropical cyclone gains strength dramati-
228 cally in a short period of time⁴⁰. This phenomenon, difficult to explain from a theoretical point of
229 view^{41,42}, results in an enhancement of the destructiveness potential of the cyclone and in a lower
230 predictability of its trajectory⁴³. Rapid intensification is usually quantified using the increment Δv
231 of maximum winds over 24h. According to this definition, a cyclone is rapidly intensifying (resp.
232 weakening) when $\Delta v > 35$ kts (resp. $\Delta v < -35$ kts). In phase space, rapid changes of the dynamics
233 correspond to approaching unstable regions of the attractor^{44,45}. Our working hypothesis is that
234 variations in the dynamical systems metrics may be able to track these transitions. Figures 6 and
235 7 show the values of (a) Δd and (b) $\Delta \theta$ associated with the rapid intensification or weakening of
236 the cyclones. The Δ are again computed over a period of 24 hours. Lateral panels show the PDFs
237 of Δd and (b) $\Delta \theta$ conditioned on the rapid weakening or intensification. In both Figures 6 and 7
238 the medians of all PDFs for rapid weakening or intensification are significantly different at the 1%
239 level under a Wilcoxon rank sum test, except for $\Delta \theta_{PV}$. Rapid intensification is associated with a
240 clear decrease of θ_{SLP} and a weak decrease of d_{PV} . In other words, there is a large coherence of
241 the dynamics of the cyclones tracked by the increased persistence of the SLP. This is accompanied
242 by a decrease of the degrees of freedom in PV. The rapid weakening displays instead a decreased
243 SLP persistence and a marked increase in d_{PV} .

244 VII. IMPLICATIONS OF THE RESULTS FOR THE NUMERICAL SIMULATION OF 245 HURRICANES

246 We now discuss our results in the framework of the dynamical systems theory established for
247 the indicators of persistence and dimensionality. From this viewpoint, high persistence and low
248 dimensional states are found at unstable fixed points of the dynamics. The link between unstable
249 fixed points and persistence has been established in theorem 4.2.7 in³¹. The theorem states that
250 the extremal index θ is smaller than 1 at periodic points and that its value depends on the degree
251 of periodicity. The physical implication of the theorem is that the more stable the state, the closer
252 the value of θ to 0. The limiting case, $\theta = 0$ corresponds to an infinite cluster length, that is the
253 dynamics never leave the state, namely an equilibrium fixed point. If instead the value is close to

254 0 but not zero, the system sticks around the state for a long time, but it will eventually leave. This
255 is a property of fixed points that have at least one unstable direction through which the system can
256 leave the neighborhood. There is no formal theorem on the connection between a low dimension
257 and fixed points, but an argument based on synchronization in³⁵. In this study the local dimension
258 is computed for spatially extended systems: Coupled Lattice Maps (CLMs). These dynamical
259 systems are characterized by a coupling by adjacent sites. In the limit for extreme coupling, the
260 CLMs have a fixed point where all the dynamics is synchronized and $d = 1$ (one particle is in
261 the state of all the others). In real systems where perfect coupling does not exist, the states of
262 low dimension d also correspond to synchronized states. For both the cases, to the best of our
263 knowledge, it has not been proved that having a low θ and d is a sufficient condition for unstable
264 fixed points. Furthermore the phase space that we use in our study is rather unusual: i) we do not
265 consider the full set of variables but only two observables that project the dynamics of the cyclones
266 on a special low dimensional subset, ii) the domain is moving and it is centered on the eye of the
267 storm; yet it is not a Lagrangian phase space, because we only follow the eye and not each single
268 fluid parcel.

269 Besides the exact mathematical meaning of our results, they are useful to highlight some prac-
270 tical aspects related to the simulation of these objects in climate and weather models. The large
271 spread of the dynamical properties obtained in tropical cyclones and the strong dependency on
272 the intensity suggests that a parametrization independent on cyclone intensity may fail to resolve
273 their dynamics, especially for intense cyclones. Parameterizations are devised for typical states
274 of tropical dynamics (isolated thunderstorms), but not specifically for the organized states of the
275 most intense tropical cyclones. Hurricanes, i.e. intense tropical cycones, would then be analogous
276 to dissipative singularities of turbulent flows⁴⁶, or *black holes* of the atmospheric dynamics⁴⁷. In
277 these cases, the physics is far from that of the average states of the system, such that adaptive
278 scaling laws and targeted parametrizations are needed. Thus, the computation of the dynamical
279 systems metrics could support the development of hurricane-specific parameterizations.

280 As a caveat, we underline that our semi-Lagrangian approach does not allow to relate the
281 present results to the predictability of the trajectories of the tropical cyclones examined in this
282 study, unlike the Eulerian approach applied to extra-tropical motions in⁹⁻¹¹. Furthermore, we
283 have used the ERA5 dataset, which has a fair but not highly-resolved representation of the con-
284 vective scales of hurricane dynamics.

285 To conclude, we have shown that the physical characteristics of tropical cyclones may be

286 understood in terms of dynamical systems metrics, which are capable of singling out peculiar
287 states of the dynamics. Our results support the idea that cyclones can be understood as being
288 reached along specific directions of the dynamics, consistent with instanton theory⁴⁸ and the no-
289 tion of melancholia states⁴⁹. This perspective opens intriguing possibilities, including the use
290 of importance sampling algorithms⁵⁰ to select simulations which approach the hurricanes states
291 as detected from the dimension–persistence analysis in the phase space. For example, in⁵¹ we
292 propose a methodology, based on dimension and persistence metrics, to reconstruct the statistics
293 of cyclone intensities in coarse-resolution datasets, where maximum wind speed and minimum
294 sea-level pressure may not be accurately represented. We conclude that the dynamical systems
295 metrics outlined here could help to address several open problems in representing the climatology
296 of cyclone dynamics and provide strategies for their parametrization and their characterization in
297 climate simulations.

298

299 **VIII. ACKNOWLEDGMENTS**

300 The authors acknowledge the support of the INSU-CNRS-LEFE-MANU grant (project DINCLIC),
301 the grant ANR-19-ERC7-0003 (BOREAS), and grant ANR- 20-CE01-0008-01 (SAMPRACE).
302 This work has received support from the European Union’s Horizon 2020 research and innovation
303 programme (Grant agreement No. 101003469, XAIDA) and from the European Research Council
304 (ERC) under the European Union’s Horizon 2020 research and innovation programme (Grant
305 agreement No. 948309, CENÆ project). B. Dubrulle was partly supported by the ANR, project
306 EXPLOIT (grant agreement No. ANR-16-CE06-0006-01).

307 **IX. DATA AVAILABILITY**

308 ERA5 data are available on the C3S Climate Data Store on regular latitude-longitude grids
309 at 0.25° x 0.25° resolution at <https://cds.climate.copernicus.eu/#!/home>, accessed on
310 2022-02-23

311

312 HURDAT2 is a database provided by NOAA and freely available at [https://www.aoml.](https://www.aoml.noaa.gov/hrd/hurdat/Data_Storm.html)
313 [noaa.gov/hrd/hurdat/Data_Storm.html](https://www.aoml.noaa.gov/hrd/hurdat/Data_Storm.html), accessed on 2022-02-23

314 **REFERENCES**

- 315 ¹A. B. Smith and R. W. Katz, “Us billion-dollar weather and climate disasters: data sources,
316 trends, accuracy and biases,” *Natural hazards* **67**, 387–410 (2013).
- 317 ²A. Grinsted, P. Ditlevsen, and J. H. Christensen, “Normalized us hurricane damage estimates
318 using area of total destruction, 1900- 2018,” *Proceedings of the National Academy of Sciences*
319 **116**, 23942–23946 (2019).
- 320 ³E. K. Chang and Y. Guo, “Is the number of north atlantic tropical cyclones significantly under-
321 estimated prior to the availability of satellite observations?” *Geophysical Research Letters* **34**
322 (2007).
- 323 ⁴J. Kossin, T. Hall, T. Knutson, K. Kunkel, R. Trapp, D. Waliser, and M. Wehner, “Extreme
324 storms,” (2017).
- 325 ⁵M. J. Roberts, J. Camp, J. Seddon, P. L. Vidale, K. Hodges, B. Vannière, J. Mecking, R. Haarsma,
326 A. Bellucci, E. Scoccimarro, *et al.*, “Projected future changes in tropical cyclones using the
327 cmip6 highresmip multimodel ensemble,” *Geophysical Research Letters* **47**, e2020GL088662
328 (2020).
- 329 ⁶E. N. Lorenz, “Can chaos and intransitivity lead to interannual variability?” *Tellus A* **42**, 378–
330 389 (1990).
- 331 ⁷S. Schubert and V. Lucarini, “Covariant lyapunov vectors of a quasi-geostrophic baroclinic
332 model: analysis of instabilities and feedbacks,” *Quarterly Journal of the Royal Meteorological*
333 *Society* **141**, 3040–3055 (2015).
- 334 ⁸C. J. Muller and D. M. Romps, “Acceleration of tropical cyclogenesis by self-aggregation feed-
335 backs,” *Proceedings of the National Academy of Sciences* **115**, 2930–2935 (2018).
- 336 ⁹D. Faranda, G. Messori, and P. Yiou, “Dynamical proxies of north atlantic predictability and
337 extremes,” *Scientific reports* **7**, 41278 (2017).
- 338 ¹⁰G. Messori, R. Caballero, and D. Faranda, “A dynamical systems approach to studying midlat-
339 itude weather extremes,” *Geophysical Research Letters* **44**, 3346–3354 (2017).
- 340 ¹¹A. Hochman, P. Alpert, T. Harpaz, H. Saaroni, and G. Messori, “A new dynamical systems
341 perspective on atmospheric predictability: Eastern mediterranean weather regimes as a case
342 study,” *Science advances* **5**, eaau0936 (2019).
- 343 ¹²A. Hochman, G. Messori, J. F. Quinting, J. G. Pinto, and C. M. Grams, “Do atlantic-european
344 weather regimes physically exist?” *Geophysical Research Letters* **48**, e2021GL095574 (2021).

- 345 ¹³M. Brunetti, J. Kasparian, and C. V  rard, “Co-existing climate attractors in a coupled aqua-
346 planet,” *Climate Dynamics* **53**, 6293–6308 (2019).
- 347 ¹⁴G. Messori and D. Faranda, “Technical note: Characterising and comparing different palaeocli-
348 mates with dynamical systems theory,” *Climate of the Past Discussions* (2020).
- 349 ¹⁵A. Gualandi, J.-P. Avouac, S. Michel, and D. Faranda, “The predictable chaos of slow earth-
350 quakes,” *Science advances* **6**, eaaz5548 (2020).
- 351 ¹⁶D. Faranda, M. C. Alvarez-Castro, G. Messori, D. Rodrigues, and P. Yiou, “The hammam effect
352 or how a warm ocean enhances large scale atmospheric predictability,” *Nature communications*
353 **10**, 1–7 (2019).
- 354 ¹⁷A. Crisanti, M. Falcioni, A. Vulpiani, and G. Paladin, “Lagrangian chaos: transport, mixing and
355 diffusion in fluids,” *La Rivista del Nuovo Cimento* (1978-1999) **14**, 1–80 (1991).
- 356 ¹⁸A. Vulpiani, *Chaos: from simple models to complex systems*, Vol. 17 (World Scientific, 2010).
- 357 ¹⁹C. W. Landsea and J. L. Franklin, “Atlantic hurricane database uncertainty and presentation of
358 a new database format,” *Monthly Weather Review* **141**, 3576–3592 (2013).
- 359 ²⁰H. Hersbach, B. Bell, P. Berrisford, S. Hirahara, A. Hor  nyi, J. Mu  noz-Sabater, J. Nicolas,
360 C. Peubey, R. Radu, D. Schepers, *et al.*, “The era5 global reanalysis,” *Quarterly Journal of the*
361 *Royal Meteorological Society* **146**, 1999–2049 (2020).
- 362 ²¹J. B. Elsner, “Tracking hurricanes,” *Bulletin of the American Meteorological Society* **84**, 353–
363 356 (2003).
- 364 ²²J. D. M  ller and M. T. Montgomery, “Tropical cyclone evolution via potential vorticity anoma-
365 lies in a three-dimensional balance model,” *Journal of the atmospheric sciences* **57**, 3366–3387
366 (2000).
- 367 ²³L. J. Shapiro, “Potential vorticity asymmetries and tropical cyclone evolution in a moist three-
368 layer model,” *Journal of the atmospheric sciences* **57**, 3645–3662 (2000).
- 369 ²⁴L. J. Shapiro and J. L. Franklin, “Potential vorticity in hurricane gloria,” *Monthly weather review*
370 **123**, 1465–1475 (1995).
- 371 ²⁵S. A. Hausman, K. V. Ooyama, and W. H. Schubert, “Potential vorticity structure of simulated
372 hurricanes,” *Journal of the atmospheric sciences* **63**, 87–108 (2006).
- 373 ²⁶K. Tory, N. Davidson, and M. Montgomery, “Prediction and diagnosis of tropical cyclone for-
374 mation in an nwp system. part iii: Diagnosis of developing and nondeveloping storms,” *Journal*
375 *of the atmospheric sciences* **64**, 3195–3213 (2007).
- 376 ²⁷T.-Y. Lee, C.-C. Wu, and R. Rios-Berrios, “The role of low-level flow direction on tropical

377 cyclone intensity changes in a moderate-sheared environment,” *Journal of the Atmospheric Sci-*
378 *ences* **78**, 2859–2877 (2021).

379 ²⁸A. R. Zhai and J. H. Jiang, “Dependence of us hurricane economic loss on maximum wind speed
380 and storm size,” *Environmental Research Letters* **9**, 064019 (2014).

381 ²⁹A. C. M. Freitas, J. M. Freitas, and M. Todd, “Hitting time statistics and extreme value theory,”
382 *Probability Theory and Related Fields* **147**, 675–710 (2010).

383 ³⁰V. Lucarini, D. Faranda, and J. Wouters, “Universal behaviour of extreme value statistics for
384 selected observables of dynamical systems,” *Journal of statistical physics* **147**, 63–73 (2012).

385 ³¹V. Lucarini, D. Faranda, J. M. M. de Freitas, M. Holland, T. Kuna, M. Nicol, M. Todd, S. Vaienti,
386 *et al.*, *Extremes and recurrence in dynamical systems* (John Wiley & Sons, 2016).

387 ³²N. R. Moloney, D. Faranda, and Y. Sato, “An overview of the extremal index,” *Chaos: An*
388 *Interdisciplinary Journal of Nonlinear Science* **29**, 022101 (2019).

389 ³³M. Süveges, “Likelihood estimation of the extremal index,” *Extremes* **10**, 41–55 (2007).

390 ³⁴N. Sarkar and B. B. Chaudhuri, “An efficient differential box-counting approach to compute
391 fractal dimension of image,” *IEEE Transactions on systems, man, and cybernetics* **24**, 115–120
392 (1994).

393 ³⁵F. M. E. Pons, G. Messori, M. C. Alvarez-Castro, and D. Faranda, “Sampling hyperspheres via
394 extreme value theory: implications for measuring attractor dimensions,” *Journal of statistical*
395 *physics* **179**, 1698–1717 (2020).

396 ³⁶D. Faranda and S. Vaienti, “Correlation dimension and phase space contraction via extreme
397 value theory,” *Chaos: An Interdisciplinary Journal of Nonlinear Science* **28**, 041103 (2018).

398 ³⁷L.-S. Young, “Dimension, entropy and lyapunov exponents,” *Ergodic theory and dynamical sys-*
399 *tems* **2**, 109–124 (1982).

400 ³⁸T. W. Anderson, “On the distribution of the two-sample cramer-von mises criterion,” *The Annals*
401 *of Mathematical Statistics* , 1148–1159 (1962).

402 ³⁹J. Molinari, D. Knight, M. Dickinson, D. Vollaro, and S. Skubis, “Potential vorticity, east-
403 erly waves, and eastern pacific tropical cyclogenesis,” *Monthly weather review* **125**, 2699–2708
404 (1997).

405 ⁴⁰F. Sanders, “Explosive cyclogenesis in the west-central north atlantic ocean, 1981–84. part i:
406 Composite structure and mean behavior,” *Monthly weather review* **114**, 1781–1794 (1986).

407 ⁴¹R. Klein, “Scale-dependent models for atmospheric flows,” *Annual review of fluid mechanics*
408 **42**, 249–274 (2010).

- 409 ⁴²A. V. Soloviev, R. Lukas, M. A. Donelan, B. K. Haus, and I. Ginis, “Is the state of the air-
410 sea interface a factor in rapid intensification and rapid decline of tropical cyclones?” *Journal of*
411 *Geophysical Research: Oceans* **122**, 10174–10183 (2017).
- 412 ⁴³C.-Y. Lee, M. K. Tippett, A. H. Sobel, and S. J. Camargo, “Rapid intensification and the bimodal
413 distribution of tropical cyclone intensity,” *Nature communications* **7**, 1–5 (2016).
- 414 ⁴⁴M. Ghil, M. D. Chekroun, and E. Simonnet, “Climate dynamics and fluid mechanics: Natural
415 variability and related uncertainties,” *Physica D: Nonlinear Phenomena* **237**, 2111–2126 (2008).
- 416 ⁴⁵H. A. Dijkstra, *Nonlinear climate dynamics* (Cambridge University Press, 2013).
- 417 ⁴⁶E.-W. Saw, D. Kuzzay, D. Faranda, A. Guittonneau, F. Daviaud, C. Wiertel-Gasquet, V. Padilla,
418 and B. Dubrulle, “Experimental characterization of extreme events of inertial dissipation in a
419 turbulent swirling flow,” *Nature communications* **7**, 1–8 (2016).
- 420 ⁴⁷J. Grover and A. Wittig, “Black hole shadows and invariant phase space structures,” *Physical*
421 *Review D* **96**, 024045 (2017).
- 422 ⁴⁸F. Bouchet, J. Laurie, and O. Zaboronski, “Langevin dynamics, large deviations and instantons
423 for the quasi-geostrophic model and two-dimensional euler equations,” *Journal of Statistical*
424 *Physics* **156**, 1066–1092 (2014).
- 425 ⁴⁹V. Lucarini and T. Bódai, “Edge states in the climate system: exploring global instabilities and
426 critical transitions,” *Nonlinearity* **30**, R32 (2017).
- 427 ⁵⁰F. Ragone, J. Wouters, and F. Bouchet, “Computation of extreme heat waves in climate models
428 using a large deviation algorithm,” *Proceedings of the National Academy of Sciences* **115**, 24–29
429 (2018).
- 430 ⁵¹D. Faranda, G. Messori, S. Bourdin, M. Vrac, S. Thao, J. Riboldi, S. Fromang, and P. Yiou,
431 “Correcting biases in tropical cyclone intensities in low-resolution datasets using dynamical
432 systems metrics, <https://hal.archives-ouvertes.fr/hal-03631098>,” (2022).

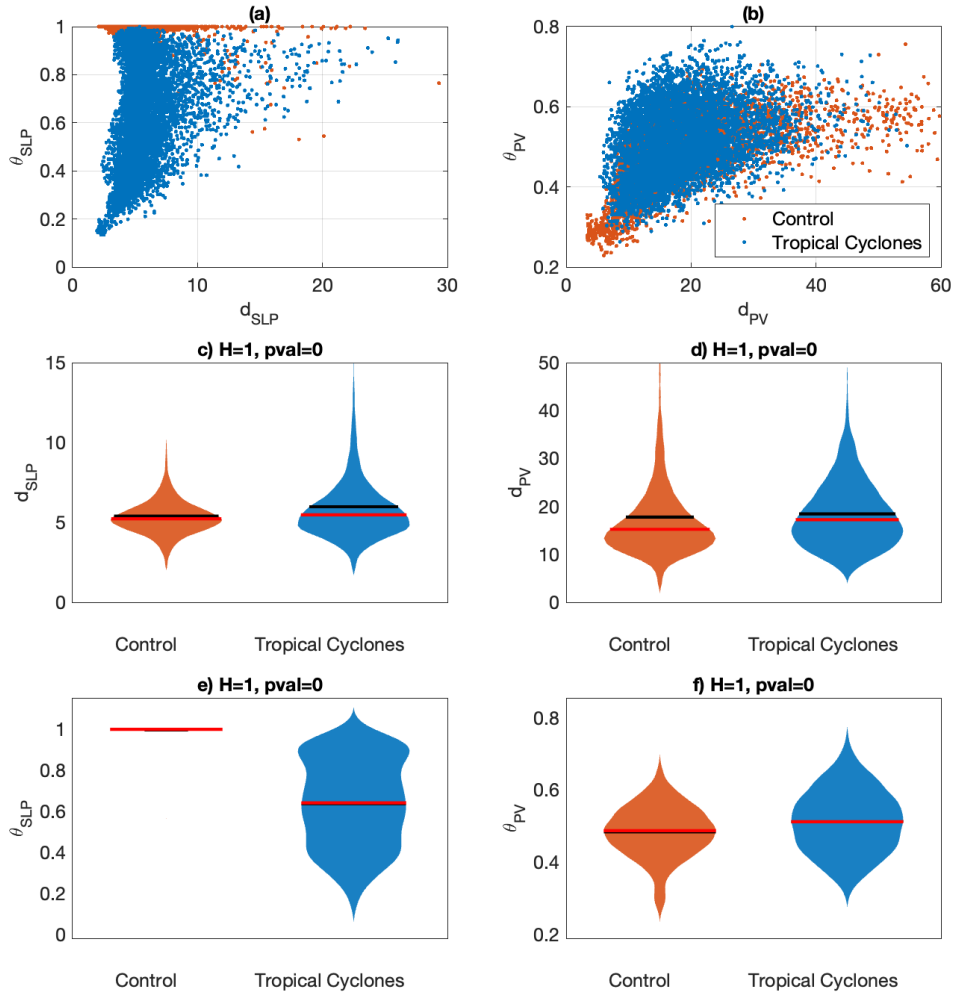


FIG. 2. Dimension d and inverse persistence θ for 6h hourly 2017-2021 ERA5 datasets on a control box [$10\text{N}<\text{lat}<20\text{N}$ $-50\text{W}<\text{lon}<40\text{W}$] (orange) and for the semilagrangian ERA5 data for tropical cyclones timesteps and center on the cyclones eye coordinates from HURDAT2 database (blue), calculated on sea-level pressure (SLP; a,c,e) and 500 hPa potential vorticity (PV; b, d,f). Panels (a,b) show the dimension-persistence diagrams; panels (c-f) show the violin plots (fatness of the patched area corresponds to the probability density) for the different dataset with the mean (red bars) and the black (medians). Note that the violin plots for the Control box in panel e) are not visible because all values are very close to 1.

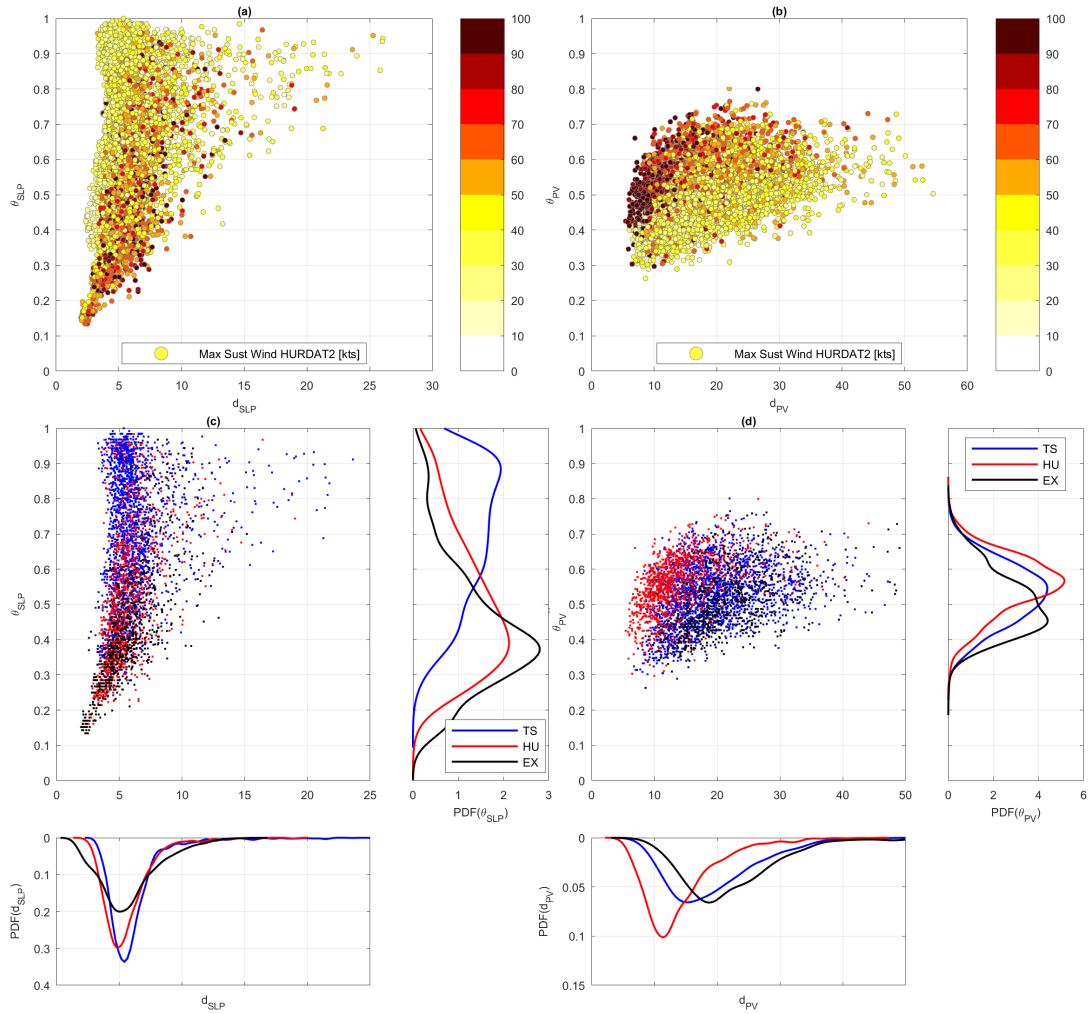


FIG. 3. Dimension d and inverse persistence θ of tropical cyclones, calculated on sea-level pressure (SLP; a,c) and 500 hPa potential vorticity (PV; b, d). The colourscales show maximum wind (a, b) and cyclone classification (c,d, see legend). Side panels show the corresponding PDFs. TS: Tropical Storm; HU: Hurricane; EX: Extratropical cyclones.

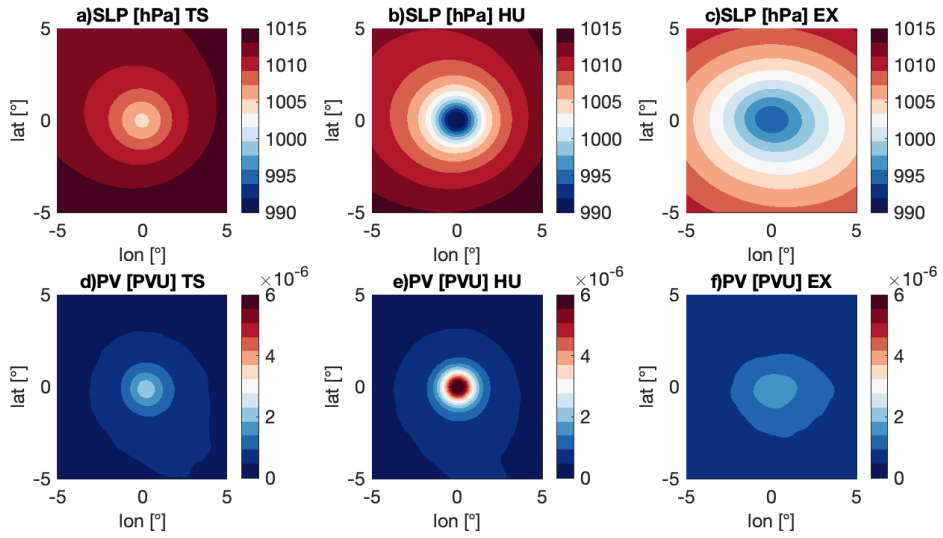


FIG. 4. Average sea-level pressure (SLP, hPa, a–c) and 500 hPa potential vorticity (PV, PVU, d–f) maps conditioned on cyclone classification (TS: Tropical Storm, a,d; HU: Hurricanes, b, e; EX: Extratropical cyclones, c,f).

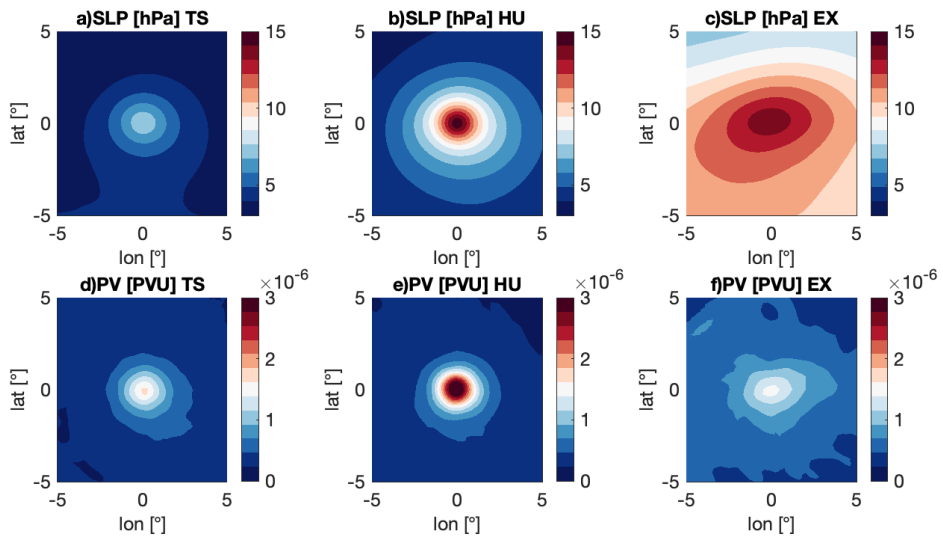


FIG. 5. Same as in Fig. 4, but for the standard deviation of the maps.

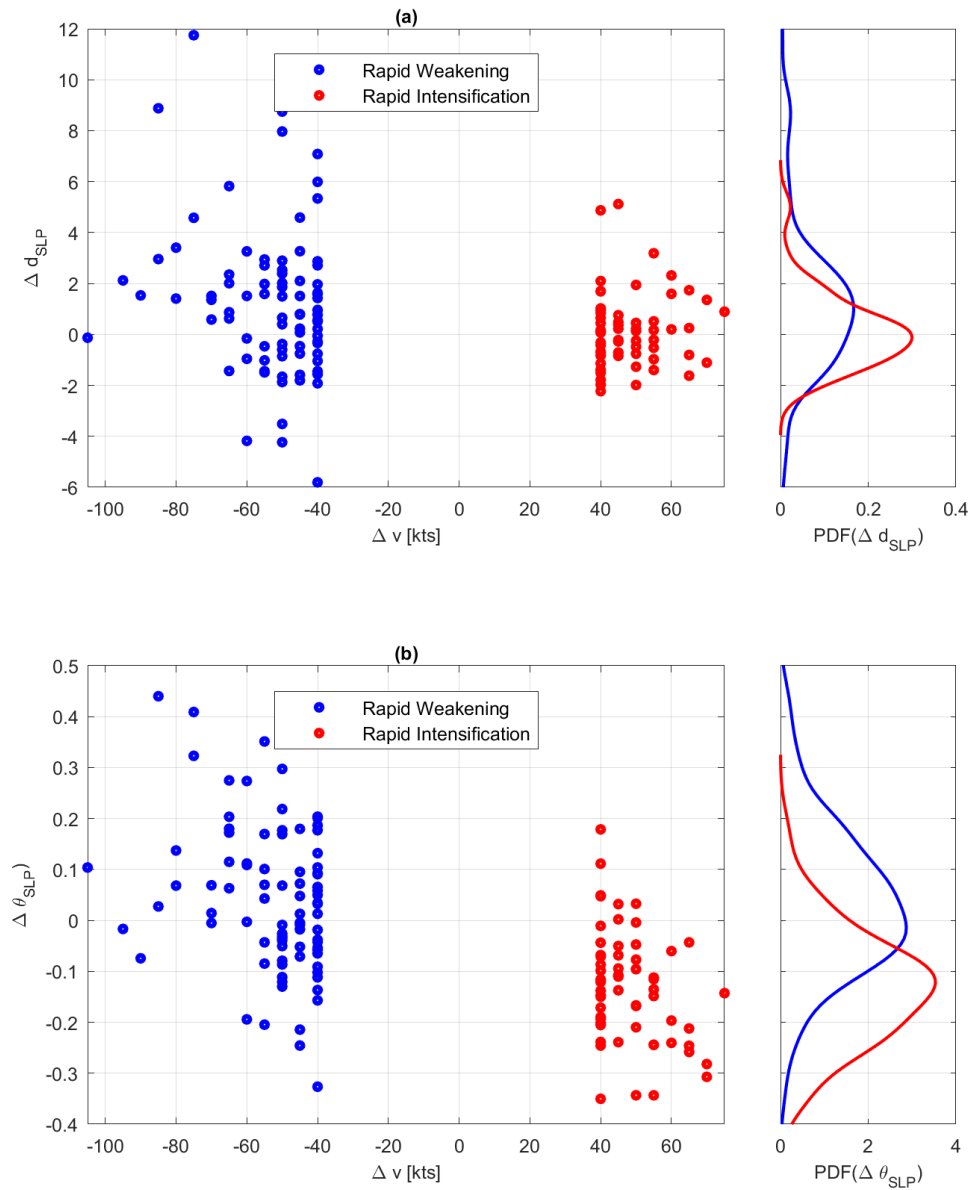


FIG. 6. 24h variation (Δ) of the dimension d (a) and of the inverse persistence θ (b) computed on SLP versus the 24h variation of maximum winds v for rapidly intensifying (blue) and rapidly weakening (red) cyclones. The side panel shows the corresponding PDFs.

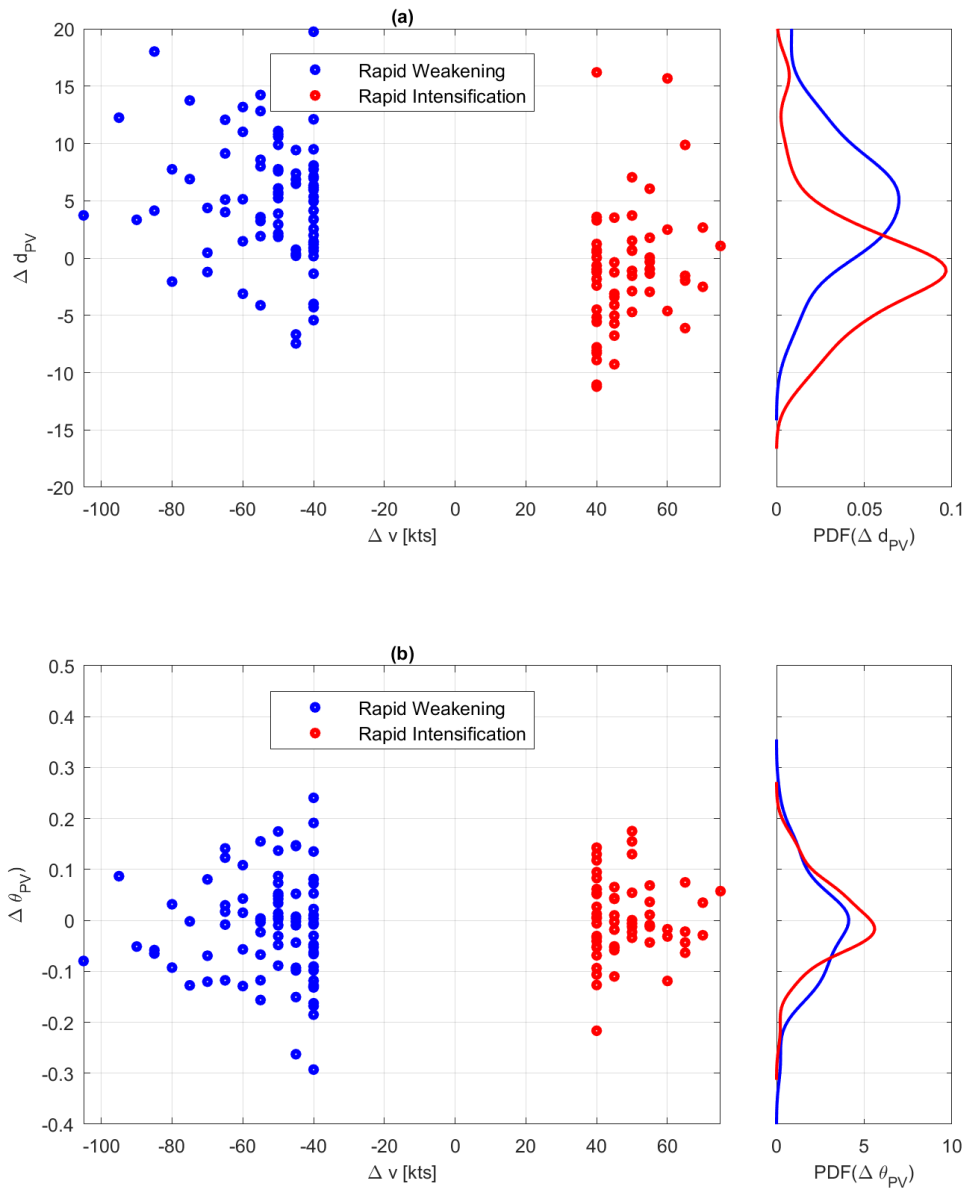


FIG. 7. Same as Fig. 6, but for d and θ computed on PV at 500 hPa.